teins were present in the cytosol. The specificity for glyphosate is high. Other common agrichemicals such as phosphinothricin, atrazine, and sulfonylureas are not acetylated by GAT (*11*).

Improved *gat* variants from the fifth iteration enabled the regeneration of glyphosate-tolerant transgenic tobacco plants. The plants were morphologically normal and fertile. To evaluate the tolerance profile of the tobacco plants, we selected T_1 plants that contained a segregating *gat* gene, using a glyphosate spray of 1 lb. acid equivalents per acre (ae/ac) and followed that with a dose-response regime using sprays of 2 to 24 lb. ae/ac. Untransformed plants showed severe symptoms or were killed by 1 lb. ae/ac (fig. S3A), whereas several transgenic GAT lines tolerated the highest dose sprayed (fig. S3B).

Fifth-iteration *gat* genes also allowed production of glyphosate-tolerant maize plants. T_0 plants were sprayed at the four-leaf stage with 104 oz./ac Roundup UltraMAX (4× field rate, equivalent to 3 lb. ae/ac glyphosate). The regenerants survived the treatment, but exhibited chlorotic banding and growth inhibition (Fig. 4B). Glyphosate tolerance improved with increases in the catalytic efficiency of GAT. With expression of seventh-iteration genes, nearly 50% of the maize regenerants showed no chlorotic banding and no growth inhibition (Fig. 4C). Most transformed plants expressing the best 10th and 11th round *gat* genes were tolerant to 6× glyphosate spray and showed no adverse symptoms (Fig. 4D). Efficacy trials of lines containing genes from several shuffling iterations are under way in the field to evaluate the commercial potential of this glyphosate tolerance trait.

Our approach shows that enzymes with useful yet insufficient activities can subsequently be improved by applying directed evolution until the desired activity is gained. DNA shuffling allowed us to develop crop plants exhibiting tolerance to the herbicide glyphosate, an important transgenic phenotype in global agriculture.

References and Notes

1. C. James, *Global Review of Commercialized Transgenic Crops: 2002 Feature Bt Maize*, International Service for the Acquisition of Agri-biotech Applications, *ISAAA Briefs*, no. 29 (ISAAA, Ithaca, NY, 2003).
2. J. E. Franz, M. K. Mao, J. A. Sikorski, *Glyphosate: A Unique Global Herbicide* (American Chemical Society, Washington, DC, 1997).
3. S. R. Padgette *et al*., in *Herbicide-Resistant Crops: Agricultural, Environmental, Economic, Regulatory, and Technical Aspects*, S. O. Duke, Ed. (CRC Press, Boca Raton, FL, 1996), pp. 53-84.
4. J. A. Gougler, D. R. Geiger, *Plant Physiol.* **68**, 668 (1981).
5. W. A. Pline, J. W. Wilcut, S. O. Duke, K. L. Edmisten, R. Wells, *J. Agric. Food Chem.* **50**, 506 (2002).
6. D. M. Stalker, K. E. McBride, L. D. Malyj, *Science* **242**, 419 (1988).
7. C. J. Thompson *et al*., *EMBO J.* **6**, 2519 (1987).
8. M. De Block *et al*., *EMBO J.* **6**, 2513 (1987).
9. G. Barry *et al*., in *Biosynthesis and Molecular Regulation of Amino Acids in Plants*, vol. 7, B. K. Singh, H. E. Flores, J. C. Shannon, Eds. (Current Topics in Plant Physiology series, American Society Plant Physiology, Rockville, MD, 1992), pp. 139–145.
10. See (*2*), p. 497.
11. Materials and methods are available as supporting material on *Science* Online.
12. S. C. Kinsky, *J. Biol. Chem.* **235**, 94 (1960).
13. E. M. Khalil, J. De Angelis, P. A. Cole, *J. Biol. Chem.* **273**, 30321 (1998).
14. The following genes were cloned by PCR on the basis of GenBank or *Bacillus* genome sequences, then expressed and assayed as described for *gat* genes in *E. coli* (*11*): M22827, *Streptomyces viridochromogenes pat*; X05822, *S. hygroscopicus bar*; M62753, *S. coelicolor bar*; D90785 ORF_ID:o273#3, *E. coli pat*; Y08559, *B. subtilis ywnH*; X06118, *E. coli rimJ*; X06117, *E. coli rimI*; U50399, *Arabidopsis thaliana HLS1*; M16183, *S. lavendulae sta*; M95912 *Saccharomyces cerevisiae mak3*; X15852, R plasmid *aacC1*; BG12054, *ydaF*; BG13164, *yjcK*; BG11421, *ykkB*; BG14128, *yvoF*.
15. Isolates B6 and DS3 were isolated by Maxygen, Inc., from local soil samples. They were identified as *B. licheniformis* on the basis of 16*S* ribosomal sequencing.
16. S. F. Altschul *et al*., *Nucleic Acids Res.* **25**, 3389 (1997).
17. F. Dyda, D. C. Klein, A. B. Hickman, *Annu. Rev. Biophys. Biomol. Struct.* **29**, 81 (2000).
18. A. F. Neuwald, D. Landsman, *Trends Biochem. Sci.* **22**, 154 (1997).
19. L. A. Castle, S. Bertain, H.-J. Cho, unpublished observations.
20. W. P. C. Stemmer, *Proc. Natl. Acad. Sci. U.S.A.* **91**, 10747 (1994).
21. A. Crameri, S.-A. Raillard, E. Bermudez, W. P. C. Stemmer, *Nature* **391**, 288 (1998).
22. J. E. Ness *et al*., *Nature Biotechnol.* **20**, 1251 (2002).
23. K. Draker, G. D. Wright, *Biochemistry* **43**, 446 (2004).
24. K. A. Scheibner, J. De Angelis, S. K. Burley, P. A. Cole, *J. Biol. Chem.* **277**, 18118 (2002).
25. Z.-Y. Zhao, W. Gu, T. Cai, D. A. Pierce, U.S. Patent 5,981,840 (2004).
26. Single-letter abbreviations for the amino acid residues are as follows: A, Ala; C, Cys; D, Asp; E, Glu; F, Phe; G, Gly; H, His; I, Ile; K, Lys; L, Leu; M, Met; N, Asn; P, Pro; Q, Gln; R, Arg; S, Ser; T, Thr; V, Val; W, Trp; and Y, Tyr.

27. We thank Y. Chen, T. Chen, L. Giver, C. Ivy, C. Krebber, G. Wu, J. Wilkinson, A. Wong, N. Trinh, A. Madrigal, A. Umthun, P. Olsen, and W. Mehre for excellent technical assistance; J. Minshull, S. Govindarajan, R. Emig, and the Maxygen bioinformatics team; D. Dagarin and A. Wadley at Byotix for the glyphosate tolerance tests with *gat* tobacco.

Supporting Online Material

www.sciencemag.org/cgi/content/full/304/5674/1151/DC1
Materials and Methods
Figs. S1 to S3
References

13 February 2004; accepted 15 April 2004

Disulfide-Dependent Multimeric Assembly of Resistin Family Hormones

Saurabh D. Patel,[1] Michael W. Rajala,[2] Luciano Rossetti,[3,4] Philipp E. Scherer,[2,3,4] Lawrence Shapiro[1,5,6*]

Resistin, founding member of the resistin-like molecule (RELM) hormone family, is secreted selectively from adipocytes and induces liver-specific antagonism of insulin action, thus providing a potential molecular link between obesity and diabetes. Crystal structures of resistin and RELMβ reveal an unusual multimeric structure. Each protomer comprises a carboxy-terminal disulfide-rich β-sandwich "head" domain and an amino-terminal α-helical "tail" segment. The α-helical segments associate to form three-stranded coiled coils, and surface-exposed interchain disulfide linkages mediate the formation of tail-to-tail hexamers. Analysis of serum samples shows that resistin circulates in two distinct assembly states, likely corresponding to hexamers and trimers. Infusion of a resistin mutant, lacking the intertrimer disulfide bonds, in pancreatic-insulin clamp studies reveals substantially more potent effects on hepatic insulin sensitivity than those observed with wild-type resistin. This result suggests that processing of the intertrimer disulfide bonds may reflect an obligatory step toward activation.

The increasing prevalence of obesity in Western societies is a cause of great medical concern (*1*, *2*). Elevated body mass index correlates with susceptibility to disease states including type II diabetes, coronary artery disease, hypertension, and dyslipidemias (*3*). Type II diabetes currently affects 17 million Americans (*4*) and has become a major public health problem. Nonetheless, the molecular basis for the link between obesity and insulin resistance—the hallmark of type II diabetes—remains unclear (*5*).

Insulin resistance in type II diabetes, and in several animal models of obesity-associated insulin resistance, can often be improved systemically by treatment with agonists for

[1]Department of Biochemistry and Molecular Biophysics, Columbia University, New York, NY 10032, USA. [2]Department of Cell Biology and [3]Department of Medicine, Division of Endocrinology and [4]Diabetes Research and Training Center, Albert Einstein College of Medicine, Bronx, NY 10461, USA. [5]Naomi Berrie Diabetes Center and [6]Edward S. Harkness Eye Institute, Columbia University, New York, NY 10032, USA.

*To whom correspondence should be addressed. E-mail: lss8@columbia.edu

the nuclear receptor peroxisome proliferator-activated receptor γ (PPARγ) (*6*–*8*). A prominent class of therapeutic PPARγ agonists is the thiazolidinediones (TZDs), which trigger improvements in insulin sensitivity in a number of different tissues, including liver, muscle, and adipose tissue (*9*, *10*). This raises the question of how functional modulation of a transcription factor, active primarily in adipocytes, can alter insulin responsiveness in diverse organs. Circulating factors secreted from adipocytes have been shown to affect insulin sensitivity in a number of different tissues [recently reviewed in (*11*)]. Thiazolidinediones and other non-TZD PPARγ agonists regulate the circulating levels of several adipokines (*12*–*14*). Resistin was identified in a number of studies (*15*–*17*), including a screen for adipocyte-specific transcripts down-regulated by treatment with TZDs (*13*).

Resistin expression levels are altered in genetic and diet-induced animal models of obesity by insulin treatment, nutritional status, and treatment with TZDs (*13*). Resistin shows no significant sequence identity to previously characterized proteins and exhibits similarity only to the other family members, RELMα, RELMβ, and the recently discovered RELMγ (*15*, *18*, *19*). All family members are characterized by ten conserved cysteine residues. Resistin and RELMβ contain an additional cysteine near their amino termini, which is conserved among species. Each resistin family member studied has a unique differential tissue distribution (*15*, *18*, *19*). Notably, whereas resistin expression in the mouse is restricted to adipocytes, RELMβ is secreted by cells in the intestinal tract. Both resistin (*13*, *20*) and RELMβ can readily be detected in plasma (*20*). Insulin- and glucose-clamp studies have shown that both resistin and RELMβ specifically blunt insulin action in the liver, resulting in reduced insulin-mediated suppression of gluconeogenesis and increased glycogenolysis (*20*). Consistent with these reports, mice lacking resistin exhibit low fasted blood glucose levels because of reduced hepatic glucose production (*21*). Notably, the effects on gluconeogenesis are opposite to those reported for the adipocyte-secreted hormone adiponectin (also called Acrp30), which increases insulin sensitivity of the same liver-specific functions (*22*).

Adiponectin has a novel structure, composed of a tumor necrosis factor (TNF)–like head domain linked to a collagenous tail (*23*, *24*). Three adiponectin protomers associate to form trimers featuring an amino terminal collagen-like domain. Two subunits of the adiponectin trimer are linked by a disulfide bond mediated by Cys22 in the collagen-like domain, and the third subunit is disulfide bonded to another trimer, forming a hexamer (*25*). Mutation of Cys22 results in trimeric structures that fail to assemble into higher order forms (*25*). Hexamers, which correspond to the low-molecular-weight (LMW) form of circulating adiponectin, provide the building blocks for the high-molecular-weight (HMW) form, which adopts a "bouquet" structure comprising 12 to 18 protomers (*25*), similar in overall structure to the complement protein C1q (*24*). Once secreted, the LMW and HMW forms of adiponectin do not interchange, and the relative amounts secreted from adipocytes are subject to regulation by insulin and other factors (*25*). TZD treatment specifically increases the proportion of HMW form secreted (*26*).

Here we show that resistin, a physiological antagonist of hepatic insulin action, adopts a complex multimeric structure strikingly similar to adiponectin: Both have forms characterized by coiled-coil trimers that form tail-to-tail hexamers through disulfide bonds near their amino termini. Furthermore, we show that, like adiponectin, resistin circulates in serum in two distinct assembly states. The disulfide-linked hexamer of resistin is the major species, but a smaller complex, lacking the amino terminal disulfide bonds is also detected. Physiological clamp studies reported here show that a cysteine mutant unable to form intertrimer disulfide bonds (Cys6Ser), and likely corresponding to the smaller complex, shows substantially higher bioactivity.

Mouse resistin and RELMβ were expressed in mammalian HEK-293T cells and purified by standard chromatographic procedures (*27*). We obtained two different crystal forms of resistin in space groups C2 and $C222_1$, and one form for RELMβ in space group I222 (table S1). Initial low-resolution phases for the $C222_1$ crystal form were obtained by a single-wavelength anomalous diffraction (SAD) experiment of a crystal derivatized with a mercury compound, mersalyl acid. These phases were augmented by phases obtained with a quick-soak bromide SAD experiment (*28*). Bijvoet difference Fourier maps derived from the native sulfur anomalous scattering were used to help in density interpretation (fig. S1). The refined structure from the $C222_1$ crystal form was used to determine the structure of the resistin C2 crystal form by molecular replacement, and the refined C2 structure was used in molecular replacement phasing of the RELMβ crystal.

Resistin and RELMβ, as expected from their high sequence identity (43% in the mature proteins), adopt similar overall structures (Fig. 1). Each protomer is composed of a disulfide-rich β-sandwich "head" domain at the C terminus linked to a helical "tail" region at the N terminus (Fig. 1A; Fig. 2, A and B). The head domain adopts a six-stranded jelly-roll topology and contains two three-stranded all-antiparallel β sheets. A DALI search (*29*) revealed no similar domains in the Protein Data Bank (PDB). However, the overall folding topology is similar to that of the C-terminal domain from octopus hemocyanin (PDB code 1js8), the only other currently known six-stranded jelly roll. The globular domain from resistin contains five disulfide bonds (Cys35-Cys88, Cys47-Cys87, Cys56-Cys73, Cys58-Cys75, and Cys62-Cys77) that are topologically conserved in the RELMβ structure. Sequence comparisons reveal complete conservation of these cysteine residues throughout the resistin family (Fig. 2A), suggesting that the disulfide pattern will be broadly conserved.

Identical multimer structures are observed in all three crystal forms (Fig. 1B). Three

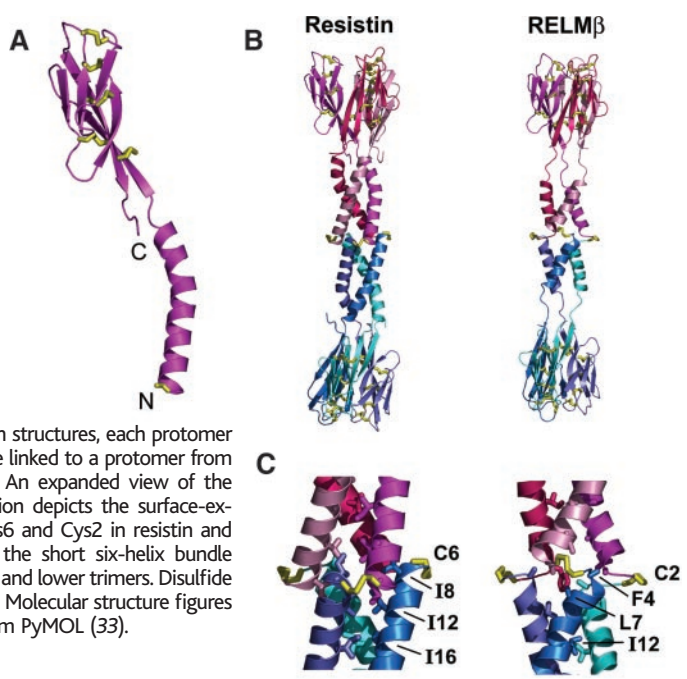

Fig. 1. Ribbon diagram representations of resistin and RELMβ. (**A**) A single resistin protomer, molecule A from the $C222_1$ crystal form, depicts the architecture of resistin family proteins, which are composed of a carboxy-terminal disulfide-rich globular domain and an amino-terminal α-helical region. (**B**) These protomers assemble to form trimer-dimer hexamers, shown for both resistin and RELMβ. In both structures, each protomer from one trimer is disulfide linked to a protomer from the associated trimer. (**C**) An expanded view of the trimer-dimer interface region depicts the surface-exposed disulfide bonds (Cys6 and Cys2 in resistin and RELMβ, respectively) and the short six-helix bundle formed between the upper and lower trimers. Disulfide bonds are drawn in yellow. Molecular structure figures are drawn with the program PyMOL (*33*).

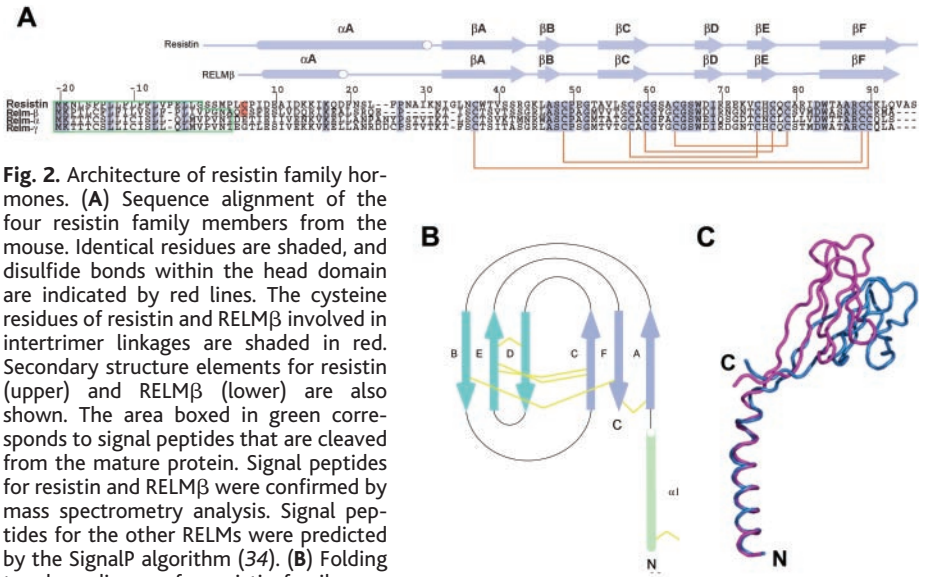

Fig. 2. Architecture of resistin family hormones. (**A**) Sequence alignment of the four resistin family members from the mouse. Identical residues are shaded, and disulfide bonds within the head domain are indicated by red lines. The cysteine residues of resistin and RELMβ involved in intertrimer linkages are shaded in red. Secondary structure elements for resistin (upper) and RELMβ (lower) are also shown. The area boxed in green corresponds to signal peptides that are cleaved from the mature protein. Signal peptides for resistin and RELMβ were confirmed by mass spectrometry analysis. Signal peptides for the other RELMs were predicted by the SignalP algorithm (*34*). (**B**) Folding topology diagram for resistin-family proteins, with disulfide bond positions drawn in yellow. The six-stranded jelly-roll topology has been found in one other structure, the C-terminal domain from octopus hemocyanin (PDB code 1js8). (**C**) The globular head domain is linked to the coil region through a flexible neck region. Superposition of two protomers from the resistin $C222_1$ crystal form, shown as α-carbon worms, depict the extent of variability in the orientation of this domain relative to the coiled coil, which varies up to 21.7° in the structures presented here.

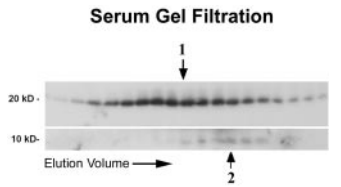

Fig. 3. Two distinct assembly states of resistin secreted from adipocytes and circulating in serum. Nonreducing Western blots of serum from wild-type mice fractionated by size-exclusion chromatography. Two overlapping elution peaks are observed. One corresponds to the major hexamer species, which runs on nonreducing gels as a covalent dimer. The less abundant peak elutes later, indicating an assembly smaller than the hexamer, and runs on nonreducing gels as a monomer, showing the lack of interchain disulfide bonds.

protomers associate through the formation of a parallel coiled coil by the amino-terminal helical regions. The β-sandwich domains do not share a large common hydrophobic core interface, as TNF family trimers do (*24*). In the $C222_1$ structure of resistin, the head domains appear to hang loosely from the helical stalk (Fig. 2C). These trimers are further interlinked to form tail-tail hexamers. To achieve this linkage, the amino-terminal coiled-coil tips from each of two trimers splay apart to enable tail-to-tail interdigitation, forming a short antiparallel six-helix bundle (Fig. 1C). Each helix from a trimer coiled coil is disulfide bonded through Cys6 (Cys2 in RELMβ) to a Cys6 (Cys2) from the opposing trimer.

For resistin, two leucine side chains from each protomer interdigitate to form the core of the short three-up/three-down six-helix bundle (Fig. 1C). The diminutive nature of this interface suggests that, but for the trimer-trimer disulfide bonds, the hexamer association would likely be unstable. For RELMβ, although electron density for the disulfide bonds is clear, nearby side chains in the six-helix bundle core are largely disordered, suggesting that they are unlikely to play a major role in stabilizing the trimer-trimer interface. Cys6 (Cys 2 in RELMβ) is conserved among resistin and RELMβ from all species, but is notably absent from RELMα. This agrees with prior observations showing that the covalent structure of RELMα is monomeric, whereas resistin and RELMβ are each covalently linked as disulfide-dependent homodimers. Furthermore, mutagenesis studies have shown that Cys6 is indeed the critical cysteine that mediates disulfide-dependent dimerization of resistin (*30*).

The interchain disulfide bonds of resistin and RELMβ are novel in that they are highly solvent when exposed, ranging from 84.6% to 89.5% solvent accessibility for RELMβ and 59.8% to 61% for the $C222_1$ crystal form of resistin (*27*). Analysis of the 24,666 disulfide bonds contained in protein structures in the PDB reveals an average solvent exposure for all disulfide bonds of 9.9%, and of 16.7% for 1,209 interchain disulfide bonds. Furthermore, the only interchain protein disulfide bonds (63 total) with solvent accessibilities >50% involve cysteine residues near the carboxy termini of artificially truncated antibody fragments. Thus, the resistin and RELMβ disulfides represent the most highly exposed disulfide bonds yet found in high-resolution structures for an intact protein.

Overall, the resistin and RELMβ structures are very similar (Fig. 1). The "head" domains have no sequence insertions or deletions relative to one another. Structure superpositions of the protomer head domains yield root mean square deviations (RMSDs) for α carbons of ~0.98 Å between resistin (residues 32 to 91) and RELMβ (residues 23 to 82). RELMβ has a shorter coiled-coil region, comprising only four turns of helix from each protomer, compared with six turns in resistin. However, the overall length of the RELMβ and resistin hexamers (each ~140 Å) is similar, as a result of an extended nonhelical "neck" region in RELMβ (Fig. 1B). The Cys6- or Cys2-mediated disulfide bonds in each complex are highly solvent exposed, but their orientations differ: In resistin, the disulfide bond from one trimer to another is made to the clockwise-adjacent protomer, as opposed to the counterclockwise-adjacent protomer in RELMβ (Fig. 1C). The threefold relationship among protomers from a single trimer is noncrystallographic in all cases. In the resistin structures, the side chains of Phe20 and Phe24 adopt similar conformations in two protomers and a substantially different orientation in the third, thus breaking the threefold symmetry of the coiled coil. This symmetry break is not seen in the RELMβ coiled coil. Mapping sequence identity of the resistin family onto the resistin or RELMβ structures shows the highest sequence variation in the coil region. Both the resistin and RELMβ complexes exhibit positive electrostatic surfaces in their "head" regions and negative electrostatic potential in their coiled-coil domains (fig. S3).

To assess the biological relevance of the novel multimeric assembly reported here, and the hexamer-forming disulfide bonds in particular, we analyzed mouse serum for the presence of hexamer and other forms of resistin. Nonreducing SDS gel analysis of medium conditioned by differentiated 3T3-L1 adipocytes (*31*) reveals a disulfide-bonded resistin dimer representing 80 to 90% of total protein, and a monomeric form lacking interchain disulfide bonds representing 10 to 20% of total resistin. Fractionation of either conditioned medium or serum by size-exclusion chromatography (Fig. 3) also revealed two distinct populations of resistin. The predominant form of resistin elutes from calibrated gel filtration columns with a calculated mass of ~54 kD and migrates as a covalent dimer on nonreducing gels (Fig. 3). The chromatographic and electrophoretic behavior of this fraction (the HMW form) is identical to that of the purified hexamer for which structures

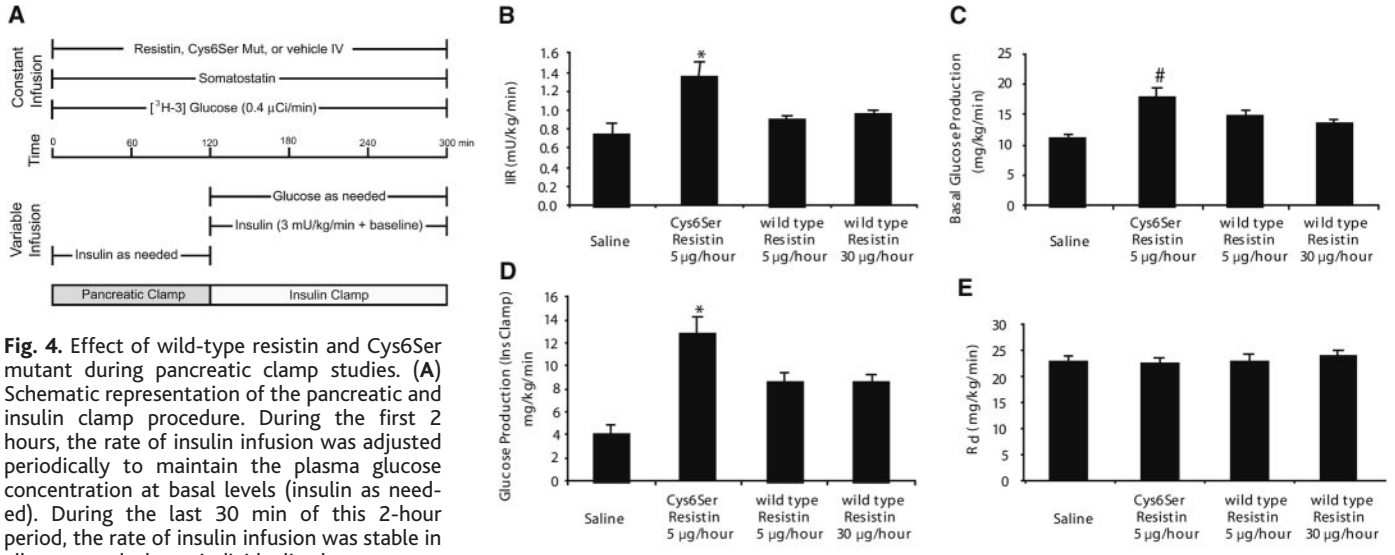

Fig. 4. Effect of wild-type resistin and Cys6Ser mutant during pancreatic clamp studies. (**A**) Schematic representation of the pancreatic and insulin clamp procedure. During the first 2 hours, the rate of insulin infusion was adjusted periodically to maintain the plasma glucose concentration at basal levels (insulin as needed). During the last 30 min of this 2-hour period, the rate of insulin infusion was stable in all rats, and these individualized rates were continued throughout the study. At the completion of the pancreatic clamp (at $t = 120$ min), an additional infusion of insulin (3 mU/kg/min) was administered to similarly raise the plasma insulin levels in all groups, and a variable infusion of a 25% glucose solution was started and periodically adjusted (glucose as needed) to maintain the plasma glucose concentration at approximately 7 mM for the rest of the study. (**B**) Rates of insulin infusion (IIR) required to maintain the plasma glucose concentrations at the basal levels. (**C**) Effects of wild-type resistin and Cys6Ser on the rate of glucose production. (**D**) Effects of wild-type resistin and Cys6Ser on the rate of glucose production under hyperinsulinemic conditions. (**E**) Effects of wild-type resistin and Cys6Ser on peripheral insulin sensitivity. Some measurements for wild-type resistin were drawn from a previous study (*20*). *, $P < 0.05$ Cys6Ser versus vehicle or wild-type resistin 5 μg/hour and 30 μg/hour; #, $P < 0.05$ versus vehicle. Sample size was at least $n = 5$ for all conditions.

were determined. 3T3-L1–conditioned media and serum also contain a second and overlapping resistin peak eluting later with a calculated mass of ~46 kD. Western blot analysis shows that this smaller species (the LMW form) migrates as a monomer on nonreducing gels, indicating that the disulfide bonds involved in hexamer stabilization are not present.

The combined observations of a smaller assembly as judged by gel filtration, the trimeric nature of noncovalent resistin assembly through coiled-coil interactions, and the absence of the critical disulfide bonds, suggest that this LMW fraction likely corresponds to a complex lacking the critical intertrimer disulfide. We note that the calculated mass for the LMW peak is greater than half that of the hexamer. However, the shapes of the resistin protein and its assemblies are highly asymmetric, and thus size-exclusion chromatography cannot be expected to yield accurate mass determinations.

To determine whether the presence of the LMW form of resistin is of biological relevance, we prepared a mutant version of resistin that lacks the critical Cys6 and has a serine residue instead, Cys6Ser. As expected, after purification from 293T cells overexpressing this mutant protein, it fails to form covalently bound dimers upon analysis with nonreducing SDS–polyacrylamide gel electrophoresis (SDS-PAGE) (*30*). We have previously used the pancreatic-insulin clamp technique to address the metabolic effects of recombinant resistin (*20*) as well as to determine the effects of the genomic ablation of the resistin gene on glucose homeostasis (*21*). A schematic representation of the experimental design is shown in Fig. 4A. Infusion of low concentrations of Cys6Ser mutant required considerably higher insulin infusion rates to sustain euglycemic conditions compared with even the high dose of wild-type resistin, indicating a higher degree of insulin resistance in the presence of Cys6Ser mutant (Fig. 4B). In line with these observations, hepatic glucose production was considerably increased (Fig. 4C), again more potently in Cys6Ser-infused animals as compared with those infused with wild-type resistin. Thus, despite elevated rates of insulin infusion, the rate of glucose production was increased by Cys6Ser infusion. At the completion of the pancreatic clamp period (at $t = 120$ min), an additional regular infusion of insulin (3 mU/kg/min) was administered to similarly raise the plasma insulin levels in all groups, and a variable infusion of a 25% glucose solution was started and periodically adjusted to maintain the plasma glucose concentration at ~7 mM for the rest of the study. Under these conditions, both wild-type and Cys6Ser-mutant resistin significantly decreased hepatic insulin sensitivity as judged by the increased hepatic glucose output. Similar to the basal conditions, the Cys6Ser mutant was substantially more potent at the low concentration than was wild-type resistin at the high concentration (Fig. 4D). Whole-body glucose disposal, however, was similar under all conditions (Fig. 4E), suggesting that both the Cys6Ser-mutant and wild-type resistin target primarily the liver.

These results are consistent with a model that LMW resistin (mimicked by the Cys6Ser mutant) is the bioactive ligand. Resistin may have to be processed to the LMW form before it can exert its bioactivity. We have proposed a similar mechanism for adiponectin based on the observation that a mutant version of adiponectin lacking a critical coiled-coil region cysteine residue (Cys22) that fails to assemble into higher order structures beyond the trimer is considerably more bioactive (*25*).

Mechanisms for regulation of assembly for adiponectin and resistin are not yet understood. However, the regulated disulfide-dependent assembly of another serum-borne protein, immunoglobulin M, is now known to involve thioredoxin-like proteins of the endoplasmic reticulum (*32*). For both adiponectin and resistin, the mutant forms lacking critical disulfide bonds in their coiled-coil domains are most active. This suggests a possible receptor-binding geometry in which the coiled-coil tails, occluded in the HMW forms and free in the mutant or processed forms, might be involved in receptor interactions.

In summary, crystal structures for resistin and RELMβ reveal hexameric assemblies consisting of trimers linked to form hexamers through highly exposed disulfide bonds at the amino termini of their coiled-coil domains. This unusual structure is suggestive of possible regulation through disulfide cleavage or by regulation during assembly. Consistent

with this is the observation of two distinct forms of resistin—the HMW hexamer and the LMW form—in serum and adipocyte-conditioned medium. The LMW form displays significantly increased bioactivity. The overall multimeric assembly of the resistin family is similar to that of adiponectin. The comparable domain architecture of these two adipocyte-specific hormones, despite diametrically opposed physiological effects, suggests a common regulatory mechanism and points to new avenues of research focusing on modulation of adipokine secretion and activity by cysteine-mediated complex formation or processing.

References and Notes

1. C. L. Ogden, K. M. Flegal, M. D. Carroll, C. L. Johnson, *JAMA* **288**, 1728 (2002).
2. K. M. Flegal, M. D. Carroll, C. L. Ogden, C. L. Johnson, *JAMA* **288**, 1723 (2002).
3. J. J. Reilly *et al*., *Arch. Dis. Child.* **88**, 748 (2003).
4. U. S. Census, *Bureau of the Census, 2000 Census Estimates;* www.cdc.gov/diabetes/pubs/estimates.htm.
5. I. M. Jazet, H. Pijl, A. E. Meinders, *Neth. J. Med.* **61**, 194 (2003).
6. T. Fujita *et al*., *Diabetes* **32**, 804 (1983).
7. T. Fujiwara, S. Yoshioka, T. Yoshioka, I. Ushiyama, H. Horikoshi, *Diabetes* **37**, 1549 (1988).
8. P. E. Beales, P. Pozzilli, *Diabetes Metab. Res. Rev.* **18**, 114 (2002).
9. H. Hauner, *Diabetes Metab. Res. Rev.* **18** (suppl. 2), S10 (2002).
10. R. R. Henry, *Endocrinol. Metab. Clin. North Am.* **26**, 553 (1997).
11. M. W. Rajala, P. E. Scherer, *Endocrinology* **144**, 3765 (2003).
12. A. H. Berg, T. P. Combs, X. Du, M. Brownlee, P. E. Scherer, *Nature Med.* **7**, 947 (2001).
13. C. M. Steppan *et al*., *Nature* **409**, 307 (2001).
14. T. P. Combs *et al*., *Endocrinology* **143**, 998 (2002).
15. I. N. Holcomb *et al*., *EMBO J.* **19**, 4046 (2000).
16. K. H. Kim, K. Lee, Y. S. Moon, H. S. Sul, *J. Biol. Chem.* **276**, 11252 (2001).
17. M. W. Rajala *et al*., *Mol. Endocrinol.* **16**, 1920 (2002).
18. C. M. Steppan *et al*., *Proc. Natl. Acad. Sci. U.S.A.* **98**, 502 (2001).
19. B. Gerstmayer *et al*., *Genomics* **81**, 588 (2003).
20. M. W. Rajala, S. Obici, P. E. Scherer, L. Rossetti, *J. Clin. Invest.* **111**, 225 (2003).
21. R. R. Banerjee *et al*., *Science* **303**, 1195 (2004).
22. T. P. Combs, A. H. Berg, S. Obici, P. E. Scherer, L. Rossetti, *J. Clin. Invest.* **108**, 1875 (2001).
23. P. E. Scherer, S. Williams, M. Fogliano, G. Baldini, H. F. Lodish, *J. Biol. Chem.* **270**, 26746 (1995).
24. L. Shapiro, P. E. Scherer, *Curr. Biol.* **8**, 335 (1998).
25. U. B. Pajvani *et al*., *J. Biol. Chem.* **278**, 9073 (2003).
26. U. B. Pajvani *et al*., *J. Biol. Chem.* **279**, 12152 (2004).
27. Materials and methods are available as supporting material on *Science* Online.
28. Z. Dauter, M. Dauter, K. R. Rajashankar, *Acta Crystallogr. D Biol. Crystallogr.* **56**, 232 (2000).
29. L. Holm, C. Sander, *Nucleic Acids Res.* **26**, 316 (1998).
30. R. R. Banerjee, M. A. Lazar, *J. Biol. Chem.* **276**, 25970 (2001).
31. D. L. Brasaemle *et al*., *J. Lipid Res.* **38**, 2249 (1997).
32. T. Anelli *et al*., *EMBO J.* **22**, 5015 (2003).
33. W. L. DeLano (2002), http://pymol.sourceforge.net
34. H. Nielsen, J. Engelbrecht, S. Brunak, G. von Heijne, *Protein Eng.* **10**, 1 (1997).

35. We thank the personnel of Advanced Photon Source (APS) beamlines 31-ID and 32-ID; National Synchrotron Light Source beamlines X4, X9, and X25; and A. Gogos and T. Boggon for help with data collection; M. Collins, A. Gogos, and D. Brasaemle for help with biochemical experiments; and F. P. Davis and A. Sali for help with solvent accessibility calculations. We also thank Z. Wang, J.-Y. Kim, and A. Narwocki for help at various stages of this project. We are grateful to W. A. Hendrickson and P. D. Kwong for critical comments. The structures reported in this paper have been deposited in the PDB as 1RFX, 1RGX, and 1RH7. This work was supported in part by grants from NIH and the Research to Prevent Blindness Foundation. Part of this work was performed as part of the National Institute of General Medical Sciences' New York Structural Genomics Research Consortium (NYSGXRC). Use of the APS was supported by the U.S. Department of Energy, Office of Science, Office of Basic Energy Science, under Contract No. W-31-109-Eng-38. Use of the SGX Collaborative Access Team (SGX-CAT) beamline facilities at sector 31 of the APS was provided by Structural GenomiX, Inc., which constructed and operates the facility.

Supporting Online Material

www.sciencemag.org/cgi/content/full/304/5674/1154/DC1
Materials and Methods
Figs. S1 to S3
Table S1
References

10 November 2003; accepted 19 April 2004

Hereditary Early-Onset Parkinson's Disease Caused by Mutations in *PINK1*

Enza Maria Valente,[1]*‡ Patrick M. Abou-Sleiman,[2]* Viviana Caputo,[1,3]† Miratul M. K. Muqit,[2,4]† Kirsten Harvey,[5] Suzana Gispert,[6] Zeeshan Ali,[6] Domenico Del Turco,[7] Anna Rita Bentivoglio,[9] Daniel G Healy,[2] Alberto Albanese,[10] Robert Nussbaum,[11] Rafael González-Maldonado,[12] Thomas Deller,[7] Sergio Salvi,[1] Pietro Cortelli,[13] William P. Gilks,[2] David S. Latchman,[4,14] Robert J. Harvey,[5] Bruno Dallapiccola,[1,3] Georg Auburger,[8]‡ Nicholas W. Wood[2]‡

Parkinson's disease (PD) is a neurodegenerative disorder characterized by degeneration of dopaminergic neurons in the substantia nigra. We previously mapped a locus for a rare familial form of PD to chromosome 1p36 (PARK6). Here we show that mutations in *PINK1* (PTEN-induced kinase 1) are associated with PARK6. We have identified two homozygous mutations affecting the PINK1 kinase domain in three consanguineous PARK6 families: a truncating nonsense mutation and a missense mutation at a highly conserved amino acid. Cell culture studies suggest that PINK1 is mitochondrially located and may exert a protective effect on the cell that is abrogated by the mutations, resulting in increased susceptibility to cellular stress. These data provide a direct molecular link between mitochondria and the pathogenesis of PD.

Parkinson's disease (PD) is a common neurodegenerative disorder that is characterized by the loss of dopaminergic neurons in the substantia nigra and the presence of cytoplasmic protein inclusions known as Lewy bodies. The majority of PD cases are sporadic; however, the identification of a number of genes responsible for rare familial forms of PD has provided important insights into the underlying mechanisms of the disease. These genes, encoding α-synuclein, parkin, UCH-L1, and DJ-1, have implicated protein misfolding, impairment of the ubiquitin-proteasome system, and oxidative stress in the pathogenesis of the disease (*1*, *2*).

We previously mapped PARK6, a locus linked to autosomal recessive, early-onset PD, to a 12.5-centimorgan (cM) region on chromosome 1p35-p36 by autozygosity mapping in a large consanguineous family from Sicily (*3*). Subsequent identification of two additional consanguineous families [one from central Italy (family IT-GR) (*4*) and one from Spain] provided additional evidence of linkage to PARK6. A critical recombination event in the Spanish family refined the candidate region to a 3.7-cM interval between flanking markers D1S2647 and D1S1539. Fine mapping of single-nucleotide polymorphisms and newly generated short tandem repeat markers in the three families defined a 2.8-megabase region of homozygosity within contig NT_004610, containing approximately 40 genes.

Candidate genes were prioritized on the basis of their putative function and expression in the central nervous system, as assessed by bioinformatic analysis and by exon amplification from a human substantia nigra cDNA library. Sequence analysis of candidate genes in affected members from each family led to the identification of two homozygous mutations in the *PTEN- induced putative kinase 1* (*PINK1*) gene. The mutations segregated with the disease phenotype in the three consanguineous families, were confirmed in the cDNA, and were absent from 400 control chromosomes, including 200 chromosomes from Sicilian individuals. The Spanish family carried a G→A